INCORPORATING SCHWANN CELLS AS A MEDIATOR OF SPINAL CORD OUTGROWTH FOR REGENERATIVE THERAPIES

By

BRIAN LAURENCE AYERS

A thesis submitted to the

School of Graduate Studies

Rutgers, The State University of New Jersey

in partial fulfillment of the requirements

for the degree of

Master of Science

Graduate Program in Biomedical Engineering

Written under the direction of

Maribel Vazquez, Ph.D.

and approved by

_____

_____

_____

New Brunswick, New Jersey

May 2020

ABSTRACT OF THE THESIS

Incorporating Schwann Cells as a Mediator of Spinal Cord Outgrowth for Regenerative Therapies

by BRIAN LAURENCE AYERS

Thesis Director:

Dr. Maribel Vazquez

There are millions of individuals who are affected by motor disabilities and peripheral neuropathy in the USA due to autoimmune disease, onset from infection, and chronic conditions. Peripheral neuropathy is a common effect of many diseases, and its prevalence is increasing with rising numbers of diabetic and obese individuals. The Schwann cell plays a key role in the physiology of the involved structures, and its regenerative capacities warrant its consideration and inclusion in mobility disorder and peripheral neuropathy therapies. Despite this, co-culture with spinal cord explants has previously been uninvestigated. This work establishes a model of the peripheral nervous system by co-culturing spinal cord explants with Schwann cells in extracellular solutions in vitro with the goal of advancing therapies for mobility and peripheral neuropathy disorders.

Acknowledgements

I would like to my advisors, Dr. Maribel Vazquez and Dr. Bonnie L. Firestein, and all members of the Vazquez and Firestein Labs. Specifically, I would like to thank Salman Khaliq, Christin Crosta, Srinivasa Gandu, and Marina Cararo Lopes of the Firestein lab and Juan Peña, Richard Cliver, Alyssa Brady, and Stephen Mut of the Vazquez lab for their assistance.

Additionally, I would additionally like to thank Nisha Singh of the Firestein lab and Juan Peña of the Vazquez lab for training me in each lab; I could not have done this without them.

Finally, I would like to thank my parents for their constant love and support for whom I owe much of my success in graduate school and life.

Some of the work herein is being prepared for publication. I would like to acknowledge the efforts of all who assisted, and continue to assist, our efforts to make this work accessible to the scientific community. Figure 1 [43], figure 2 [43], and figure 7 [37] were reproduced with permission from previous work and publications of the Vazquez lab.

Table of Contents

List of Illustrations

1. Background

1.1 Health Impact of Mobility Disorders and Peripheral Neuropathy

There are millions of individuals who are affected by motor disabilities and peripheral neuropathy in the USA due to autoimmune disease, onset from infection, and chronic conditions.[1,2,3] Many of these diseases affect both the central and peripheral nervous systems, but their clinical presentation can solely affect the peripheral nervous system.[4] Peripheral neuropathy is a common effect of many diseases, and its prevalence is increasing with rising numbers of diabetic and obese individuals.[5] Loss of sensation in peripheral neuropathy has been shown to be a true risk factor for the likelihood of sustaining a fall when comorbidities are controlled for which may be due to impairment in vibratory sense and unipedal balance.[6] Falls can cause further injury that creates additional problems with mobility and decreased independence. Loss of sensation from peripheral neuropathy can cause trauma to go unnoticed and ulcers which can lead to infection.[7] This can lead to increased hospitalization and decreased quality of life. Peripheral neuropathy results from dysfunction along the nerve and at the neuromuscular junction (NMJ) with great heterogeneity of mechanistic causes.[8] The Schwann cell (ShC) plays a key role in the physiology of these structures, and its regenerative capacities warrant its consideration and inclusion in mobility disorder and peripheral neuropathy therapies.

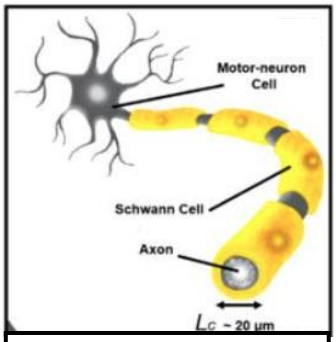

Figure 1: Myelinating Schwann Cells. A motor neuron cell (grey) that has its axon myelinated by the myelinating Schwann cell type. Taken from citation 43.

1.2 Role of Schwann Cells in the Peripheral Nervous System

Schwann cells serve two predominant roles in the mature nervous system: myelinating nerves (Figure 1) and capping the neuromuscular junction (Figure 2). Nerve myelination is critical for rapid saltatory conduction of motor and some sensory nerve fibers, and failure of Schwann cells to myelinate these nerves will lead to peripheral neuropathy and mobility disorders.[9] The neuromuscular junction is a tripartite synapse (Figure 2) consisting of lower motor neurons, skeletal muscle, and Schwann cells (ShC) that controls voluntary movement through the release of acetylcholine across the synaptic cleft.[10-12] Schwann cells also possess powerful regenerative capabilities such as creating glial bridges for connecting damaged neuronal connections to functional neurons, transdifferentiating between myelinating and NMJ capping ShC types, secreting regulatory neurotrophins to injured neurons, and guiding the growth of nerves to their targets after injury.[13-17] Comparatively few NMJ models include glial cells in any way.[18]

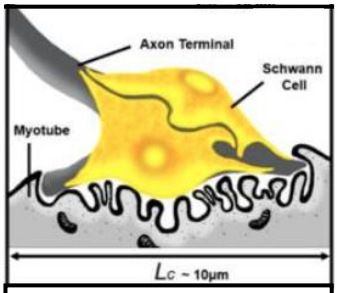

Figure 2: Terminal Schwann Cells An axon terminal (darker grey) terminal synapsed with a myotube that are capped by the NMJ capping Schwann cell type. Taken from citation 43.

1.3 Advancing Peripheral Nervous System Therapies in vitro

In vitro systems can be used to expand basic science knowledge and inform animal and clinical studies. It is often desirable to emulate the in vivo environment as much as possible to accomplish this. In vitro models have been used to analyze axon regeneration, and microfluidic systems have been shown to mimic the in vivo environment better than conventional in vitro systems.[19,20] The development of the NMJ has been studied using a variety of models,[21-29] but the contribution of Schwann cells has been largely ignored in NMJ literature.[30]

Models that include organotypic components can be used to bring the complexity of in vivo cellular systems into the dish to recapitulate their behavior.[31] Co-cultures of

explants with relevant cell types can also partially enhance in vivo recapitulation.[32] Some co-cultures that have been performed include dorsal root ganglion (DRG)::ShC, DRG::oligodendrocytes, central nervous system neuron::oligodendrocyte, and spinal cord explants (SCE)::astrocyte.[33,34] However, a SCE::ShC culture is as of yet unexamined, and these in vitro cellular models are more representative of central nervous system.

Moreover, the risk reward profile of testing ShC therapies in human subjects can be unfavorable to their clinical implementation further highlighting the need for robust in vitro models that can assay the potential therapeutic roles of Schwann cells for these diseases in controlled in vivo mimicking environments. We believe we can advance work on mobility disorders and peripheral neuropathy with controlled microfluidic environments incorporating Schwann cells.

1.4 Current Project

The synergy between the labs of Doctors Maribel Vazuez and Bonnie L. Firestein provide an advantage for developing such a model. The Vazquez lab has shown improved growth and viability of a lower motor neuron::myotube culture when ShC are included, and the Firestein lab has examined neuronal::muscle responses using co-cultures of spinal cord explants and cultured myotubes on microelectrode arrays for lab-on-a-chip applications.[35-37] This work will continue and combine those research thrusts by examining SCE::ShC interaction in microfluidic volumes within several media types.

The S-42 ShC line was chosen from prior work in the Vazquez lab to model terminal ShC because their behavior is similar to that of primary ShC and they express key glial markers.[37] SCE are useful for investigating questions about the in vivo environment that animal studies would have trouble probing because they bring some of that biological complexity into the dish with them. The S42 cell line is cultured with Dulbecco's Modified Eagle Medium (DMEM) while SCE are frequently grown in Neurobasal. Elliot's B solution

is a clinically used and FDA approved cerebrospinal fluid mimic that closely matches the pH, electrolyte composition, glucose content, and osmolarity of cerebrospinal fluid,[38] and therefore may serve as a valuable component in recapitulating the in vivo environment. This work will look at the effect of Schwann cell density on spinal cord explant outgrowth with the goal of advancing in vitro Schwann cell peripheral nervous system models.

2. Methods and Materials

2.1 Schwann Cell Model

The Schwann cell component used for the SCE::ShC model was the S-42 cell line. ShC were cultured at 37 ˚C, 95% humidity, and 5% CO2. (Figure 3) The surface tension of new flasks was broken by adding Dulbecco's Modified Eagle Medium (DMEM) with 10% FBS. Cells were passaged from T-75 flasks by washing with Dulbecco's Phosphate Buffered Saline for 6-8 minutes before being dislodged with Accutase for 3 minutes. The cells were then centrifuged in 15 mL tubes for 3 minutes at 1500 RPM. Media was replaced every 2-3 days or at the first sign of a change in the hue of the DMEM or the presence of "floaters." Flasks were passaged about 85% confluency. Flasks were allowed to grow more confluent for some tests to obtain higher cell densities.

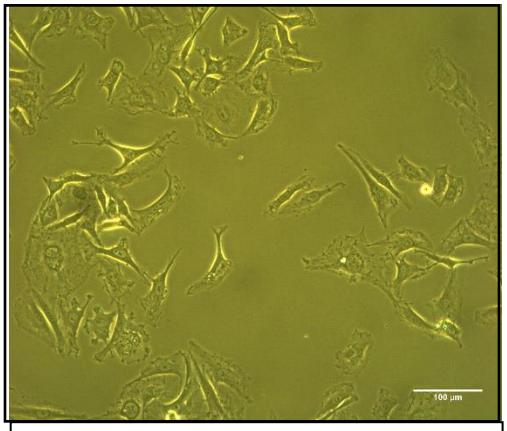

Figure 3: ShC culture in DMEM (10% FBS) at 24 hours.

2.2 Spinal Cord Explant Dissection

Spinal cord slices were dissected from embryonic day 17 and 18 rats that were extracted via Cesarean section (IACUC protocol number: PROTO99990080). Dissections were performed in Gay's Balanced salt solution (1% of 30 μM kynurenic acid and 0.6% glucose solution). In brief, embryos were decapitated with forceps, a dorsal incision was made along the midline of the body from cephalad to caudal to at a depth just superficial to the spinal cord, and spinal cords were extracted by their lumbar and, if necessary, cervical ends. (Figure 4 A,B) Spinal cord was sliced to thicknesses of 250-300 μm using a McIlwain Tissue Chopper after removing excess dissection media from spinal cord with a P1000 pipette. (Figure 4 C) Ends of SCE were removed from chopping disc and remaining SCE slices were rinsed into a one inch petri dish with HBSS. Of ethical importance, the SCE used in this work were all taken from rats that were to be used in other work in the Firestein lab, ie, no extra animals were harmed or sacrificed for this work.

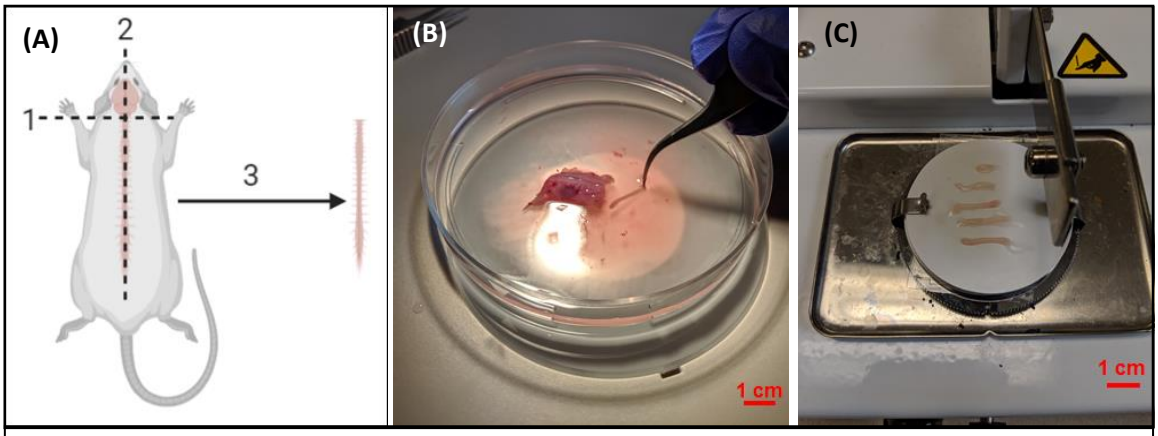

Figure 4: Spinal cord explant dissection: (A) A schematic of the spinal cord extraction. A dorsal incision is made along the midline of the body from cephalad to caudal (2) and the spinal cord is removed (3). **(B)** An image of the spinal cord being removed from an embryo with forceps (3). **(C)** Spinal cords placed on chopping disc of the McIlwain tissue chopper prior to removal of dissection media and chopping.

2.3 Microfluidic Systems

2.3.1 Modified Campenot Chambers

Robert Campenot invented compartmentalized chambers for examining neurite growth between cells separated by a barrier in 1977.[39] The specific design of the modified Campenot chambers utilized in this project consists of a circular central chamber with a diameter of 1 cm, circumscribed by a microarray of channels that are 3 µm tall, 10 µm wide, and 200 µm long, with a separation distance of 50 µm that connect to outer chambers surrounding outer perimeter of the circular array.[40] Devices are fabricated with polydimethylsiloxane PDMS elastomeric molding and lift off. Devices were incubated overnight with laminin 30 µg/ml.

2.3.2 Spinal Cord Observation Ring Enclosure (SCORE)

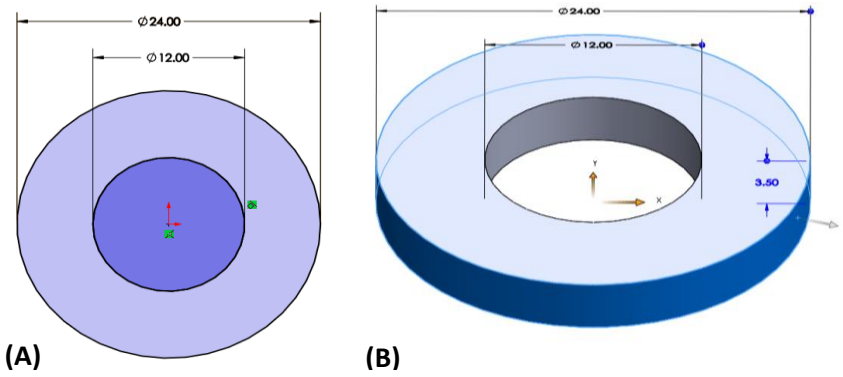

Figure 5: Schematic showing the dimensions of the SCORE from a: (A) Top view showing dimensions of 12 mm chamber concentric with 24 mm outer perimeter. **(B)** an alternate view

Novel devices were designed and fabricated from PDMS to enhance and improve some aspects of the modified Campenot chambers. The spinal cord observation ring enclosure (SCORE) consists of a single circular 12mm diameter chamber that is concentric with an outer 24 mm chamber that constitutes the outer boundary of the device. (Figure 5) The SCORE was designed in order to improve the loading, viability, and imaging of the spinal cord explant outgrowth by simplified setting that still recapitulates the environment of other PDMS microfluidic devices. Devices were incubated overnight with laminin 30 µg/ml.

2.3.3 Elastomeric Molding

Polydimethylsiloxane (PDMS) was mixed in a 9:1 ratio of elastomer : curing agent and measured by volume in 50 mL syringes. Solution was degassed under vacuum to remove all bubbles, poured onto a silanized wafer wrapped in foil, degassed again to remove bubbles formed during pouring, and baked at 60 ˚C overnight. After removing foil from cured PDMS/wafer, PDMS was peeled off wafer and devices were removed from PDMS with biopsy punches. Devices were cleaned with 70% ethanol and bonded to slides by applying corona ejection to slide and device for 20 seconds and pressed together.

2.4 Conventional in vitro Systems

24 well plates were utilized to further enhance positive aspects of the SCORE experimental design. 24 well plates are well studied culture systems that provide the ability to investigate cellular systems in microfluidic volumes cultures prior to incorporating them in microfluidic devices. Devices were incubated overnight with laminin 30 µg/ml.

2.5 Solutions to Mimic Extracellular Fluid

Cultures were performed in three media types: Dulbecco's Modified Eagle Medium, Neurobasal, and Elliot's B Solution, all with 10% FBS and 2% penicillin-streptomycin. Neurobasal was also supplemented with B27 0.5 mM Glutamax. All media types contain inorganic salts and glucose in varying concentrations. Neurobasal and DMEM contain additionally contain amino acids and vitamins. Neurobasal and DMEM are commonly used culture media in research practice. Elliot's B Solution (Figure 6) is supplied in 10 mL ampules, and it is FDA approved as a diluent for intrathecal lumbar injections to treat meningeal leukemia and

Figure 6: Elliot's B Solution. A single 10 mL glass ampule of Elliot's B solution prior to having been opened.

lymphocytic lymphoma. After the ampule is unsealed, the Elliot's B Solution is filtered to remove any glass particulate.

2.6 Schwann Cell Morphology

Schwann cell proliferation rate and cell shape index (CSI) were quantified over a 24 hour period. CSI is a dimensionless measure that captures cell morphology by taking a ratio of the area (A) to the perimeter (P) calculated as show in Eqn. 1:

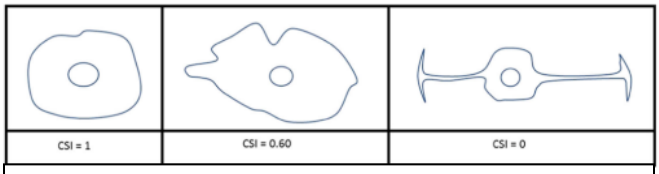

Figure 7: Schematic of a cell's morphology as it corresponds to CSI. A very round cell with a CSI of 1 **(left)** becomes less rounded **(middle)** and eventually elongated with a CSI of zero **(right)** as time passes. Figure taken from citation 37.

$$\mathrm{CSI} = \frac{4\pi \mathrm{A}}{\mathrm{P}^2}$$

where a CSI of 0 indicates a very elongated cell while a CSI of 1 indicates a round cell as indicated in Figure 7.[40] This provides a baseline measure of cellular behavior and assurance that the microfluidic environment has not caused significant changes on that behavior.

Spinal cord explant viability was assessed visually as viable explants show much greater opacity than necrotic tissue.

2.7 Spinal Cord Explant Outgrowth

Spinal cord explant outgrowth was quantified and assessed by several methods including:

2.7.1 Rectangular Method

Outgrowth was measured by drawing a rectangle with sides parallel to the image border intersecting the points of outgrowth furthest away from the body of the SCE. (Figure 8A) The vertical (top to bottom) and horizontal (side to side) distances of the

rectangle were taken to be the diameters of an elliptical object. Outgrowth was then quantified as the average of the two diameters.

2.7.2 Ellipse Fit method

SCE are commonly measured as ellipses.[41] SCE outgrowth was manually segmented by selecting points around the periphery of the outgrowth and ellipses were fitted to them with the method developed by Fisher et al.[42] This generates an ellipse (Figure 8B) with measures of area, perimeter, and diameters better oriented with the SCE outgrowth than the rectangular method, which can be used to quantify elongation of outgrowth. Elongation of the outgrowth was calculated as shown in equation 2:

$$E = 1 - \frac{R_{minor}}{R_{major}}$$

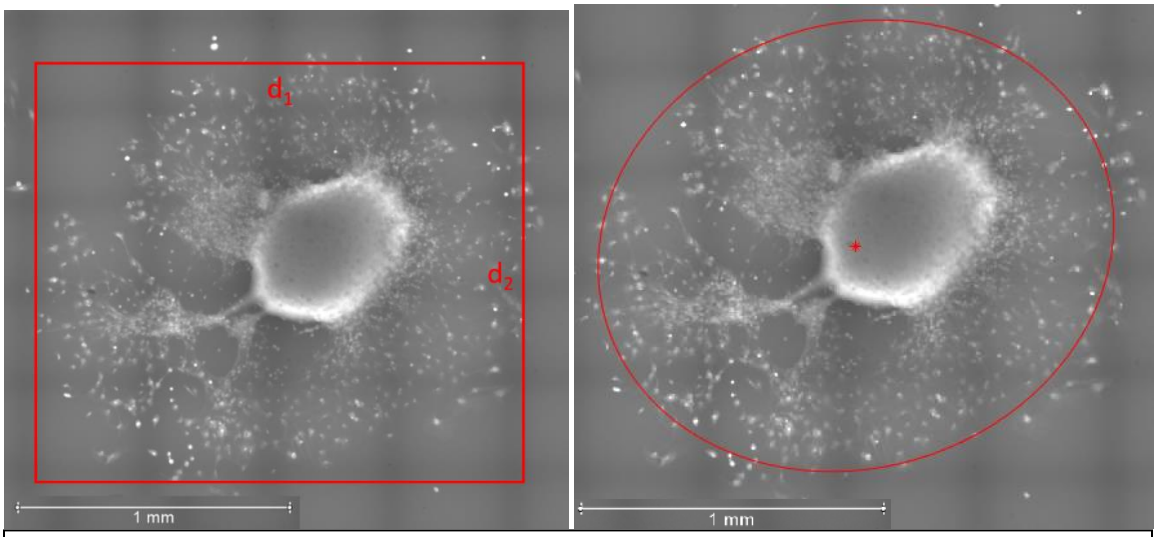

Figure 8: Schematic of Outgrowth Measure Methods: (Left) a SCE measured by the rectangular method of calculating ellipse diameters. **(Right)** the same SCE measured by the ellipse fit method**.**

3. Results and Discussion

3.1 Overview of Experiments Performed

The following experiments were performed to collect data on the interaction between spinal cord explant (SCE) to Schwann cell (ShC) co-culture in extracellular solutions. ShC were cultured in flasks with DMEM, Neurobasal, and Elliot's B Solution to observe

their effect on Schwann cell behavior. SCE and ShC were co-cultured in modified Campenot chambers in Neurobasal and DMEM to investigate the effect of extracellular fluid on SCE outgrowth and viability. SCE were co-cultured with ShC at 2 densities in modified Campenot chambers in Neurobasal to determine the effect of these densities on SCE outgrowth and viability. SCE were co-cultured with ShC at 4 densities in the SCORE in Neurobasal to further determine the effect of Schwann cell density on SCE outgrowth and viability. SCE were co-cultured with ShC at 4 densities in 24 well plates in Neurobasal and Elliot's B Solution to further investigate the effect of the extracellular solutions and ShC density on SCE outgrowth and viability.

3.2 Schwann Cell Growth and Behavior in Extracellular Solution

Schwann cells were cultured in Dulbecco's Modified Eagle Medium, Neurobasal, and Elliot's B Solution. Their CSI and proliferation rate were compared across the three media at 24 hours. Differences in CSI were statistically insignificant across media types at zero and 24 hours. (Figure 9A). Proliferation was similar between Neurobasal and DMEM as shown by their similar percent increase over 24 hours, but Elliot's B Solution increased by ~15% less than Neurobasal and DMEM over the same period. (Figure 9B) This is likely due to the presence of amino acids and vitamins present in Neurobasal and DMEM that Elliot's B Solution lacks. These data show the S42's are viable in all three media types.

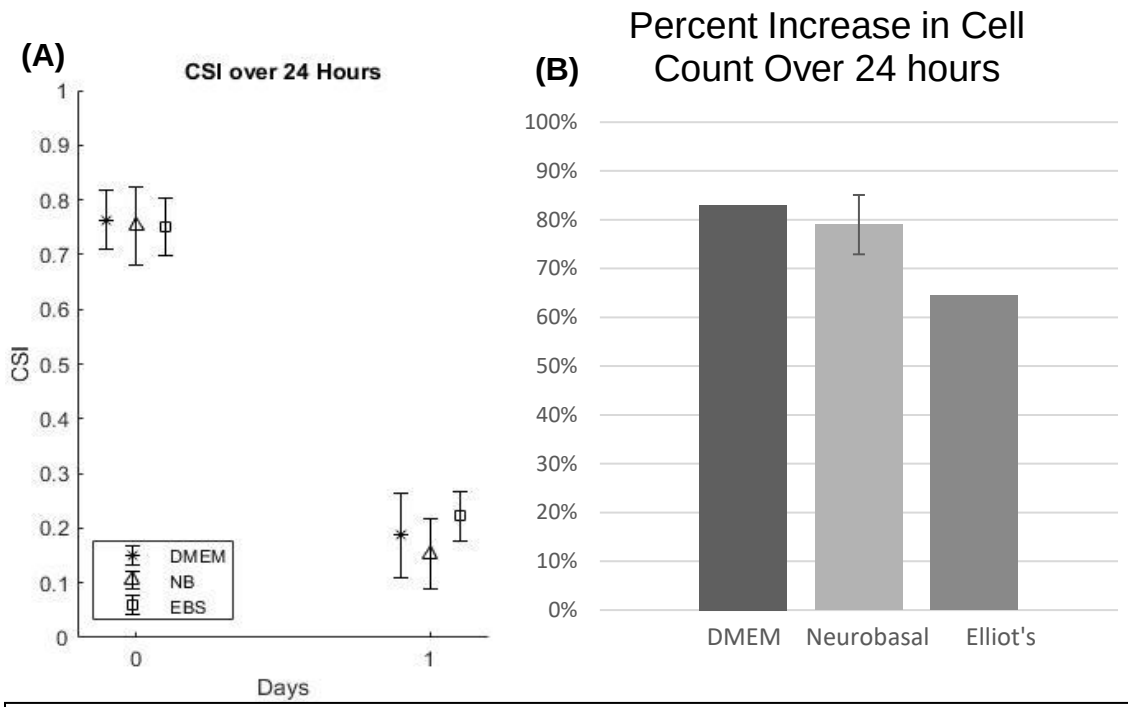

Figure 9: Measures of Schwann cell behavior in DMEM, Neurobasal, and Elliot's B Solution. (A) CSI measured at 0 and 24 hours. No statistical difference was seen between media types at each time point. **(B)** Schwann cells in Elliot's B Solution proliferated by ~15% less than Neurobasal and DMEM over the same 24 hour period.

3.3 Spinal Cord Explants and Schwann Cells in Modified Campenot Chambers with DMEM and Neurobasal

Embryonic day 17 SCE and ShC were co-cultured in the modified Campenot chambers in Neurobasal and DMEM. Five SCE were cultured per condition. By DIV 7, three of the SCE in Neurobasal produced extension while no SCE were found to produce extensions in DMEM. (Figure 10)

While some SCE did display outgrowth, only one had an observable level of translucence that could be considered very healthy (Figure 11A,B). This same explant had markedly greater outgrowth as compared to other explants with extensions. (eg Figure 11C,D) It is unclear what caused the difference in outgrowth between the SCE.

Based on the results of this experiment, and those from the comparison of media solutions on ShC growth, it was concluded that the Neurobasal formulation was the better choice for the hybrid SCE:ShC model. This is a logical choice as the SCE is the far more complex component of the system.

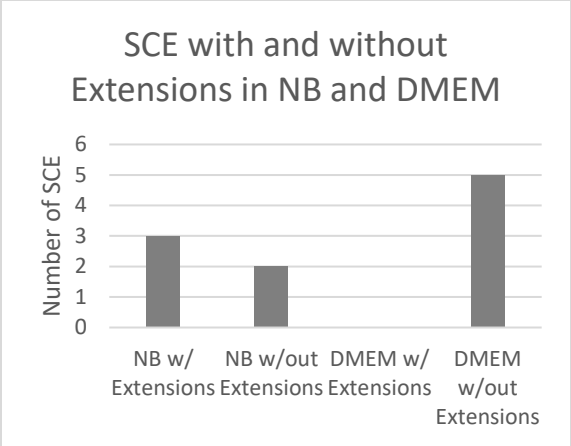

Figure 10: SCE with and without Extensions in Neurobasal (NB) and Dulbecco's Modified Eagle Medium (DMEM). Three out of five SCE grown in Neurobasal produced some level of outgrowth while those in DMEM were not observed to produce any.

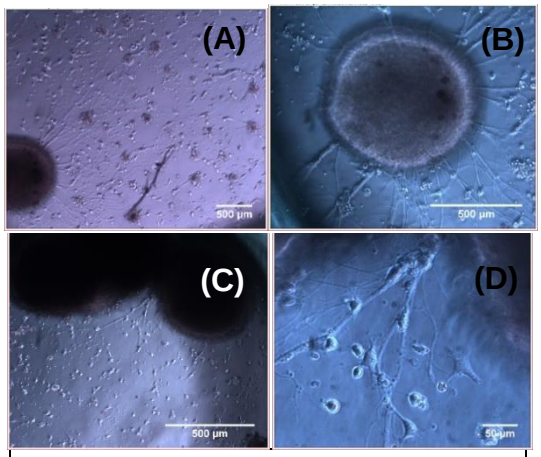

Figure 11: SCE in Neurobasal. (A) The healthiest SCE with the most outgrowth in Neurobasal. **(B)** Inset of (A). **(C)** A less healthy SCE with extension in Neurobasal. Note that the shadow of the reservoir wall makes the explant darker in appearance. **(D)** Inset of (C).

3.4 Spinal Cord Explants and Schwann Cells in Modified Campenot Chambers with Neurobasal

Embryonic day 18 SCE were co-cultured with Neurobasal in the modified Campenot chambers at 2 densities, one on the lower order of 10^6 cells/mL and one on

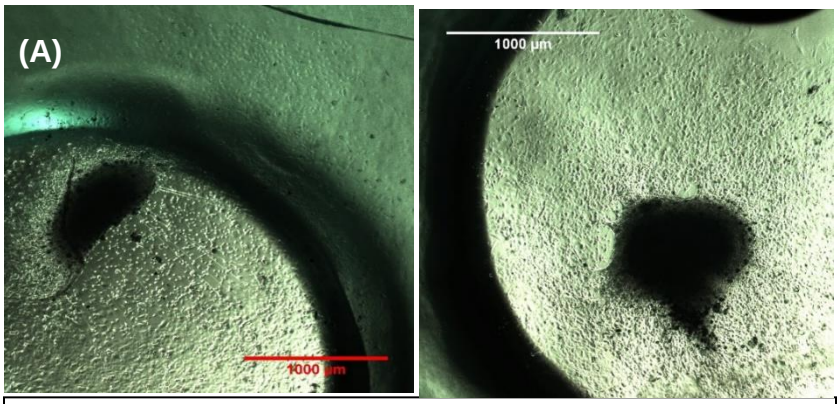

Figure 12: SCE in the lower [ShC] with Neurobasal at DIV 8. (A) SCE with observable axon-like extensions along ventral portion. **(B)** SCE with more uniform outgrowth containing lower diameter extensions.

the upper order of 10^4 cells/mL. ShC were loaded 3 days prior to the loading of the SCE. Three SCE were loaded per [ShC] on DIV 1. While the SCE with a [ShC] on the order of 10^6 showed poor or no outgrowth and viability by DIV 4, SCE in the lower density condition displayed outgrowth at the same time point. This could be due to the timing at which the SCE were exposed to different concentrations of the ShC as they proliferated which work from the Vazquez lab has previously shown in a primary cell in vitro model.[40] However, it is more likely that a microenvironment occlusion effect was caused by too great of a Schwann cell destiny that caused the SCE at the higher concentration to perform more poorly. The three SCE that were loaded to the low Schwann cell density exhibited different forms of outgrowth. (Figure 12)

There were additional problems with the modified Campenot chambers that made them less than ideally suited for these experiments. Loading and positioning the explants with the ventral portion facing the microarray at a relatively proximal distance was difficult due to the circulation of fluid flow within the chamber and reservoir. Shadows from the reservoir walls could make imaging all portions of the SCE and outgrowth difficult and positioning a SCE near the array necessitates a reservoir in the same vicinity. The outgrowth of the SCE was also not nearly as observable through the PDMS of the devices as were the portions exposed to the open reservoir top. These issues were addressed with the design of a novel device that would also facilitate observing and promote a better understanding of the interaction between the ShC and the SCE.

3.5 Spinal Cord Explants and Schwann Cells in Modified Campenot Chambers with Neurobasal in SCORE with Neurobasal

The Spinal Cord Observation Ring Enclosure (SCORE) was designed with the purpose of creating a more controlled experimental environment that would maximize the ability to view SCE outgrowth while still being cultured on the same substrate surrounded by PDMS. (Figure 13) SCE were loaded to the SCORE with ShC at

densities of $2.8*10^6$, $1.4*10^6$, $6.9*10^5$, and 0 cells/mL, so that the concentration of Schwann cells would span down the from upper range of the previous experiment. All SCE co-cultured with ShC exhibited some level of outgrowth by DIV 2 while the SCE in the no ShC condition appeared far darker and did not exhibit outgrowth. (Figure 14) This supports the idea that the SCE in the higher density ShC condition were less viable due to a combined effect from the device and the density. Moreover, outgrowth began at earlier time points for densities on the same order as the prior Campenot chamber experiment which further points to a relationship between Schwann cell density and the culturing device on the time course of SCE development.

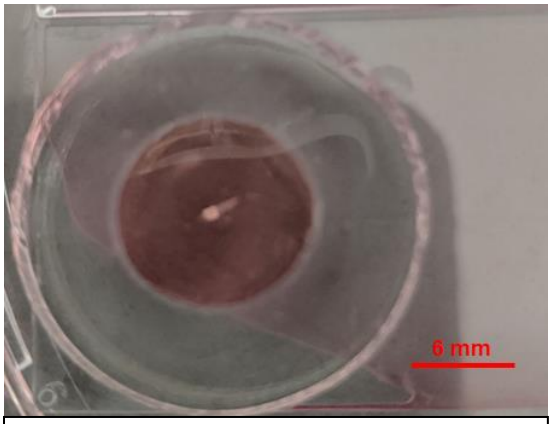

Figure 13: A spinal cord explant in the SCORE. This design facilitated imaging of outgrowth while culturing the SCE in the same materials as typical PDMS microdevices**.**

The most robust outgrowth came from a SCE with the highest ShC density (Figure 14A,B), but a pattern between ShC and robustness of outgrowth could not be concluded. Density of extensions was also noted to thin between DIV 2 and 3 which could be a result of pruning or decreased viability. The SCORE device was successful in meeting the need of improving SCE loading and outgrowth observation, but there were problems

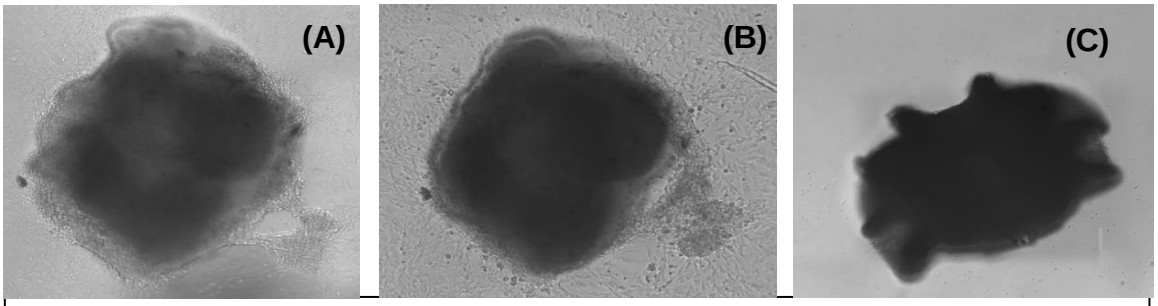

Figure 14: SCE inside SCORE with Neurobasal. (A) High [ShC] SCE DIV 2 that exhibited the most robust outgrowth. **(B)** The same SCE looking less viable on DIV 3. **(C)** A SCE without ShC with much darker appearance and no outgrowth on DIV 1.

balancing media evaporation with height. Adding a sufficient volume of fluid to stop the devices from drying out likely led to too great of a diffusion length for the SCE. This makes determining the effect of Schwann cell density on SCE viability or potential pruning behavior inconclusive.

3.6 Spinal Cord Explants and Schwann Cells in Modified Campenot Chambers with Neurobasal in 24 Well Plates in Elliot's B Solution and Neurobasal

To further control the microfluidic environment, 24 well plates were used to determine what effect ShC density had on outgrowth. Four densities of Schwann cells with greater separation from each other were used: $7.16*10^6$ cells/mL, $5.97*10^5$ cells/mL, $9.94*10^4$ cells/mL, and 0 cells/mL. The high density ShC condition is greater than previous densities used and the lowest is on par with the lowest density used to this point. This shows how Schwann cell density can affect outgrowth over a greater range than the previous experiments.

3.6.1 Rectangular Method

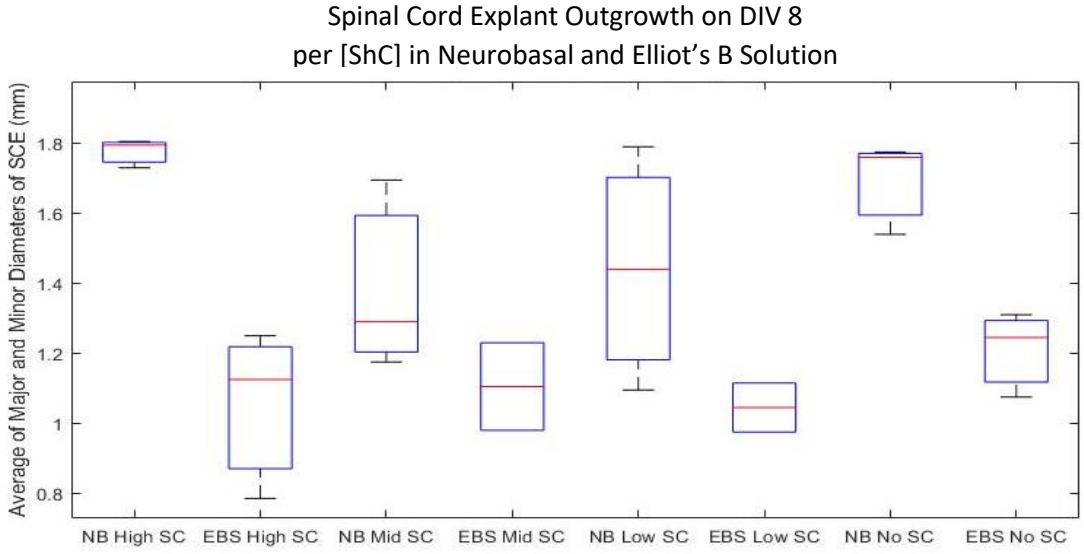

Figure 15: SCE outgrowth in 24 well plates for all [ShC] as measured by the rectangular method in Neurobasal and Elliot's B Solution at DIV 8. The figure shows box and whisker plots with median and outliers for each media type and [ShC]. [ShC] did not have a statistically significant effect on outgrowth within media types, but media type did have a statistically significant impact as per one-way ANOVA.

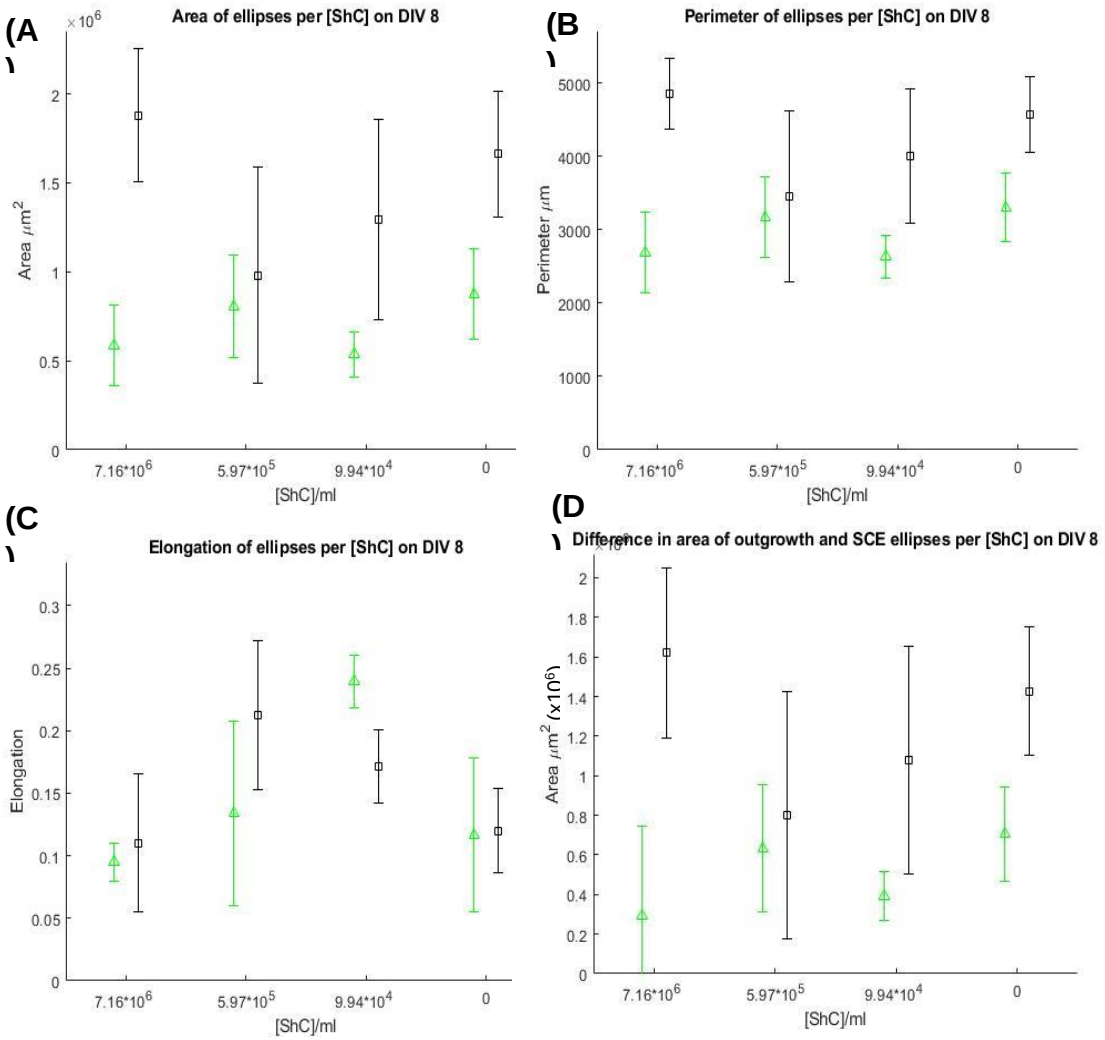

Figure 16: Average and standard deviation of SCE outgrowth in 24 well plates for all [ShC] as measured by the ellipse fit method in Neurobasal (black squares) and Elliot's B Solution (green triangles) at DIV 8 for: (A) Area in millions of micrometers^2. [ShC] did not have a statistically significant effect on outgrowth within media types, but media type did have a statistically significant impact as per one-way ANOVA. **(B)** Perimeter in micrometers. [ShC] did not have a statistically significant effect on outgrowth within media types, but media type did have a statistically significant impact as per one-way ANOVA. The similarity to (A) demonstrates ellipses were bing calculated similarly across SCE. **(C)** Elongation calculated as shown in equation 2. Note increase in maximum elongation across middle [ShC]'s, but statistical significance was not shown as per one-way ANOVA **(D)** Area of outgrowth minus the area of SCE in millions of micrometers^2. Note similarity of data to (A) showing the lack of initial SCE area on maximum outgrowth area. [ShC] did not have a statistically significant effect on outgrowth within media types, but media type did have a statistically significant impact as per one-way ANOVA.

Outgrowth was greater in Neurobasal than EBS as shown in Figures 15 and 16. This difference is not necessarily surprising as the Neurobasal formulation includes vitamins, amino acids, and B27. No observable trend was established with regards to [ShC] on outgrowth. (Figure 15)

The similarity in outgrowth of the high and no [ShC] condition and increased viability further suggest that there is an upper limit to the [ShC] that should be added in SCE co-culture to the modified Campenot chambers.

3.6.2 Ellipse Fit Method

SCE outgrowth was manually segmented and fitted to an ellipse using a method amended from Haines et al.[44] that utilizes MATLAB code published by Fisher et al.[45] An example of the output can be seen in Figure 8B.

The area and perimeter of outgrowth calculated from the fitted ellipse yielded similar results to the outgrowth results from the rectangular analysis with regards to the effect of [ShC]. However, the elongation of the SCE group at the 10^5 ShC/mL density in Neurobasal had a higher elongation than its counterparts. This elongation is suggestive of an optimal ShC density for producing outgrowth that may be more indicative of more mature SCE as outgrowth from the SCE is not uniform in vivo. SCE area also did not influence outgrowth area as shown by the similarity between outgrowth area (Figure 16A) and SCE area subtracted from outgrowth area (Figure 16D).

3.6.3. Further Discussion of 24 Well Plate Results

Although the cell tracker fluorescence was a necessary component for obtaining the outgrowth results, it led to an additional problem. Cell tracker had to be removed to observe fluorescence over time, but this sometimes led to the unfortunate lift off of the SCE from their substrate. The problems with SCE lifting off may have been increased due to the change in substrate, glass to plastic.

The similarity in outgrowth of the high and no [ShC] condition in this experiment, and the results from the SCORE, further suggest that there is an upper limit to the [ShC] that should be added to microfluidic devices if their growth cannot be met with the appropriate introduction of necessary molecules to survive.

While the neurobasal media led to superior results with regards to maximum outgrowth, Elliot's B Solution still yielded viable SCE with outgrowth. This is not necessarily negative as some applications with EBS may preferentially limit SCE outgrowth, such as intrathecal lumbar injections for meningeal leukemia or lymphocytic lymphoma. Moreover, Elliot's B Solution could play an important role for further in vitro work distinguishing differences between intrathecal and direct-to-site of injury injections. These results may be an effect of Schwann cell location relative to the SCE. Previous work from the Vazquez lab has shown increased cellular viability and extension of lower motor neurons when ShC were cultured across a microchannel array.[37] This suggests that the signals the neurons receive from the ShC and how they are interpreted could be distance and context dependent.

4. Conclusion

This work is an appropriate next step in advancing the in vitro microfluidic culture models that the Vazquez and Firestein labs have previously produced as a tripartite hybrid spinal cord explant, skeletal muscle, and Schwann cell model will enable the in vitro investigation of a more physiologically relevant cellular system. Although maximum outgrowth was lower in Elliot's B solution than Neurobasal, this can be beneficial depending on whether outgrowth is desired for a given application as Elliot's B solution is a diluent for cancer treatment and Neurobasal is made for optimal research culture conditions.

The knowledge that there is an upper limit to the ShC density that can be co-cultured with SCE in some devices will help guide future designs. The apparent time dependence

of SCE outgrowth from ShC addition further elucidates previous work from the Vazquez lab and should be considered in future studies. Although there is no effect on maximum outgrowth as a function of ShC density, there may be an effect on the morphology of outgrowth. This information will be used to develop controlled microfluidic models of the peripheral nervous system that will enable further investigation of this work.

5. Future Directions

The enhanced understanding of the type of outgrowth we can expect from the SCE, how this outgrowth and ShC interact, and the problems to confront with the design of a microfluidic system for this model will enable future work to better investigate more specific questions with regards to the cellular model. Immunohistochemistry will be performed for Tau 46 to stain axons and S100B to stain Schwann cells. Additionally, stains for molecules of specific fiber types, such as for acetylcholine receptors of motor axons, will elucidate which neurological pathways in the spinal cord systems are exhibiting outgrowth.

We are much more prepared to move the experimental system back into microfluidic devices with channel arrays. Optimization of a microfluidic system will enhance further investigation of the effect of ShC::SCE co-culture and will enable the analysis of the time dependent addition of ShC in more controlled conditions. The addition of fluid flow to the system will facilitate more robust cultures. Fluid flow will empower research to investigate the introduction of controlled concentrations and volumes of damage and therapeutic molecular cues for specific injurious and degenerative peripheral nervous system models.

6. Appendix- Background of Schwann Cell Transdifferentiation and Regenerative Capabilities

Schwann cell (ShC) progenitors originate at the neural crest in embryonic development and form ShC precursors that give rise to melanocytes, endoneurial fibroblasts, parasympathetic neurons, and immature ShC.[44] By embryonic day 18 in rat species, the organization of ShC and axon structures within peripheral nervous system fascicles mature away from an organization similar to that of the central nervous system and begin to exhibit blood vessels, collagen, extracellular matrix, early perineurium, myelinating ShC surrounding axon families (groups of axons prior to individual axon myelination), Schwann cell precursors (SCP) that have become immature ShC, and a change in the maturity of ShC molecular markers which demonstrates a transition to an organization that is much closer to that of adult nerves.[45] In the following days before birth, Schwann cells balance proliferation and death to make a 1:1 ratio of ensheathing ShC to individual axons as axon families begin to radially sort.[46] Immature ShC become several types of mature ShC such as myelinating Schwann cells, non-myelinating Remak Schwann cells, and terminal ShC that cap the neuromuscular junction (NMJ) depending on the axon fiber type they encounter in radial sorting.[47,48]

ShC that undergo denervation after transection are demyelinated, but they are not identical to the aforementioned ShC types.[49] Denervated ShC are like immature Schwann cells in that they do not myelinate, but they upregulate adhesion molecules such as N-Cadherin and integrin α1β1.[50] Moreover, Remak ShC do not express P0 while denervated and immature Schwann cells do.[51] Axon ensheathing Schwann cells include myelinating ShC as well as non-myelinating Remak ShC which are critical in nerve and axon development, regeneration, maintenance, and metabolism.[47] 10-15% of non-myelinating axons are ensheathed in rodents and nearly all of these fibers are

ensheathed in humans.[51] Remak bundles of unmyelinated sensory C-fibers transmit pain signals to the central nervous system and their disruption can cause neuropathic pain even without injury. For example, loss of the gene Gabbr1 in Remak ShC leads to an increase in the number of these pain transmitting fibers which causes painful hypersensitivity to thermal and mechanical stimuli and impaired coordination of locomotion.[47] Improper myelination of fibers seen in conditions like diabetes mellitus and Charcot-Marie-Tooth disease result in peripheral neuropathy which cause pain, sensory deficits, and degeneration and loss of axonal fibers.[52,53]

Myelinating Schwann cells are the most well-known and best studied type of Schwann cell. Myelination is a process balanced by separate transcriptional programs consisting of positive and negative regulators.[51] Differences in molecules expressed and their levels, such as low levels of Neuregulin 1 (NRG1) in ensheathed axons and high levels in myelinated axons, help communicate the proper function ShC should adopt.[54] Low levels of NRG1 cause hypomyelination, and high levels cause hypermyelination of axons that should be myelinated.[55] Mice deficient for NRG1 have sensory axons that are insufficiently myelinated, but viral transfection of the gene restores myelination showing NRG1 is essential for myelination.[55] Interestingly, other evidence has shown NRG1 may also have a role in denervation and is not required for myelin maintenance suggesting that its function is dependent upon a variety of conditions.[51] Deficiencies of beta-site amyloid precursor protein-cleaving enzyme 1 result in unprocessed NRG1 which causes hypomyelination and dysregulation of radial axonal sorting due to dysfunction of myelination and not the sorting process itself.[56]

Proper timing of immature ShC myelination in development is mediated by transcription factors Oct-6 and Brn2.[51] Myelination additionally needs continuing signaling to be maintained. Krox-20 is a transcription factor that is necessary for myelin gene activation capable of forcing the abandonment of the cell cycle, prevention of

apoptosis, and the abolishment immature ShC marker expression.[51] The knockout of Krox-20 results in alterations of the 1:1 ShC:axon ratio of radial sorting in development as myelination is altered.[57] Krox-20 stabilizes myelination by suppressing c-Jun in Schwann cells (a major repressor of myelination), decreasing ShC proliferation in response to NRG1, and blocking cell death from TGFβ.[58] Cyclic adenosine monophosphate (cAMP) is involved in the activation of normal myelination and is mediated by the transcription factors NFκB and CREB.[59] Steroid hormones including progesterone, glial derived neurotrophic factor (GDNF), and brain derived neurotrophic factor (BDNF), and insulin-like growth factor have also induce myelination.[51]

The myelination state of the Schwann cell is also susceptible to destabilization. Notch is a transcription factor that represses myelin maintenance postnatally, mediates the transition of SCP to immature ShC, and is suppressed by Krox-20.[51] Forced expression in ShC represses myelin production by cAMP and delays myelination postnatally; overexpression accelerates demyelination and dedifferentiation regardless of the presence of an injury.[60,61] Neurotrophin 3 (NT3) decreases myelin, P0, and myelin associated glycoprotein (MAG) levels.[51] Pax-3 is expressed and inhibited by cAMP signaling in immature and mature non-myelinating ShC, but forced expression down regulates cAMP itself as well as Krox-20 but not N-Cadherin or L1.[62] Pax-3 expression by itself is capable of inhibiting apoptosis by TGFβ1, and it also has roles in ShC dedifferentiation, survival, and proliferation.[63] P38 mitogen activated protein kinase (MAPK) mediates myelin degradation by NRG and FGF-2, and its inhibition stops demyelination and dedifferentiation.[64] P38 MAPK forced expression can prevents cAMP and Krox-20 expression, causes dedifferentiation of ShC to an immature phenotype, and induces c-Jun.[64] C-Jun is the primary suppressor of myelin expression by Krox-20 and cAMP, induces several of the aforementioned myelination inhibitors, and is rapidly expressed after nerve injury leading to ShC dedifferentiation.[65]

Wallerian degeneration (WD) is the cascade of events including axonal loss, macrophage infiltration, phagocytosis of myelin sheathes, Schwann cell proliferation, and dedifferentiation in response to nerve injury.[51] Successful WD is marked by expedient initaiton and termination as well as proper signaling between ShC, macrophages, fibroblasts, and endothelial cells.[66] ShC are characterized by novel phenotypes that utilize many of the same signaling pathways but are ultimately unique in their overlap of implementation.[46] The state of Schwann cell myelination exercises considerable control over the events in Wallerian degeneration and axonal regeneration. C-Jun holds powerful roles inducing trophic factors, altering adhesion molecules expression, myelin clearance, and activation of a reparative program in ShC.[67,68] Suppression of c-Jun in ShC impairs axon regeneration, increases neuronal death, decreases neurotrophic factor production, and results in dysfunctional repair and recovery.[68] Sox-2 co regulation with c-Jun, Pax-3, and Notch also assist in the demyelination process. [51]

ERK1/2 is up regulated after transection leading to macrophage recruitment by monocyte chemoattractant protein-1 (MCP-1) which is further enhanced by signaling from TNF-α and leukemia inhibitory factor (LIF) from ShC.[51] ShC initiate myelin clearance displaying some phagocytotic activities similar to that of macrophages until macrophages have been sufficiently recruited to take over myelin debris removal.[51,69] ShC up regulate the expression of surface adhesion proteins including N-CAM, Ng-CAM/L1, N-cadherin, and L2/HNK-1 and extracellular matrix molecules like laminin and fibronectin.[70] Transection of the nerve also initiates Ephrin type-B receptor 2 (Eph2B) signaling between ShC and fibroblasts which manifests in cell sorting and collective migration from the distal stump across the injury gap; loss of Eph2B signaling leads to disorganized migration and misoriented axonal extension.[71] The expression of neurotrophic factors such as BDNF, GDNF, and IGF-1 are increased which is

suppressed when ShC meet the proximal stump leading to the development of a gradient that decreases across the injury gap in a distal to proximal manner directing axonal growth along it.[72] After the nerve is cut, axons do not always reach their targets depending on the lesion distance thought which is thought to be due the loss of the reparative ShC phenotype.[73] This has been recapitulated and enhanced with GDNF transfected ShC seeded conduits in a rat sciatic nerve model.[74] If an axon successfully bridges the lesion, it will take on the myelination state it possessed prior to injury demonstrating some form of transcriptional memory.[75]

There are further distinctions between motor and sensory axon fiber types. Schwann cells from sensory and motor nerves differentially express cell adhesion molecules that likely contributes to the proper guidance to their appropriate organs.[72] Specifically, ShC that were connected to motor nerves preferentially express L2/HNK1 epitope while sensory neurons preferentially express NCAM.[76,77] Though this expression is lost after transection, ShC may exhibit some preference to express the cellular adhesion molecule type they had previously produced.[78,77] Denervated cutaneous nerves that were able to reinnervate their targets have been shown to preferentially express mRNA for the growth factors BDNF, NGF, VEGF, and IGF-1 while ventral root motor nerves express GDNF and pleiotrophin at greater amounts.[79]

Motor nerves present additional challenges in proper nerve regeneration and reinnervation. After a critical window of time post injury in a mouse model of sciatic nerve crush injury, motor axons that reached the skeletal muscle motor end plate at the NMJ did not reinnervate while sensory axons did.[80] The same study showed human subjects with peripheral nerve injury who received decompression surgery sooner after injury exhibited return of sensation but motor improvement was limited.[80] A rat sciatic nerve model of transection injury has shown somewhat contradictory results where increased duration of denervation prior to suture of the defect corresponded to lower numbers of

reinnervated motor units, but axons that did meet the NMJ reinnervated regardless of denervation duration.[81] This raises the question of the extent of heterogeneity between the motor systems of different species. Evolutionary demands placed upon different species has led to differences in cellular and functional recovery capacity such as greater redundancy of motor pathways in rat allowing the rerouting of motor inputs and feedback, the increased size of primate motor tracts may limit plasticity in their motor system, and the ability of these fibers to reorganize based on these differences.[82] Post injury, terminal ShC concentrate acetyl choline receptors at motor end plate as increased density of the receptor increases signaling to axons to innervate the motor end plate, but this function of the reparative program is much shorter in duration in the mammalian nervous system than in frogs which coincides with enhanced recovery.[83]

The presence of terminal Schwann cells at NMJ is on of the biggest distinctions between sensory and motor fibers. NMJ changes after injury show latency depending on the distance from nerve transection, but sign of WD begin to occur within a 24 hour period when ShC infiltrate the synapse to phagocytize debris whereas ShC proliferation and number at the NMJ occur later with increase of exposure to axonal NRG increase and NT3, respectively.[83] Terminal ShC produce Stromal Derived Factor-1 in response to induction by α-latrotoxin after axon terminal insult which binds the CXCR4 receptor increases the restoration of synaptic signaling and the growth of motor axons from the ventral spinal cord.[84] The ShC extend processes that link end plates and provide axons a path to extend upon, so, if one motor endplate forms a NMJ with an axon, the same axon is more likely to defasciculate and synapse with adjacent motor end plates.[83] This causes axons to synapse with different muscle fibers and leave some dennervated which leads to axon sprouting along the substrate created by other terminal Schwann cells extending from other motor end plates, but terminal Schwann cells apoptose to conclude the clearance of debris from the synapses which reduces their number of ShC

that attract axons towards the motor end plate.[83] Delays in reinnervation ultimately lead to impaired regeneration and recovery.[73] Stable ShC are repelled from the synaptic cleft as to not interfere with acetylcholine release and diffusion across the cleft by laminin-β-2 which is expressed in the basal lamina only at the synaptic cleft; its deletion leads to the invasion into the synaptic cleft and impaired synaptic transmission across the NMJ.[83]

The interplay of some of these dynamics can be seen in a study of rat spinal cord transection. Transection of spinal cord in rat caused a subset of NMJ in lower leg flexors to sprout nerve terminals and disassemble their synapse by week two which reassembled by month two with continued terminal sprouting.[85] Another subset of NMJ in lower leg flexors maintained terminals without sprouting, but they exhibited decreasing concentrations of acetyl choline receptors.[85] Yet another subset of flexors and most extensors of the lower leg had minimal alterations.[85] Further interruption of afferent connections did not increase instability of the unstable subsets, but exercise decreased the number of unstable synapses showing that the vulnerability of a particular NMJ to disruption is based on the likelihood the muscle is inactive after injury.[85] The study did not look at roles of ShC but could be important as they are an active partner in coordinating NMJ synaptic transmission.

Age then becomes a factor as rehabilitative measures are easier to implement in the younger portion of patient population. A study in mice has shown that the age of ShC in ShC-seeded nerve grafts was the determining factor in motor reinnervation regardless of ShC to host age mismatch providing further reason to consider age in regenerative therapies.[86] This is a positive result in some sense, but it does raise the consideration that older patients would require allogeneic grafts (requiring human leukocyte antigen and innate immune system matching concerns) or if their ShC could be reprogrammed ex vivo to create grafts with greater ShC plasticity from their own tissue.

7. Bibliography

1. Wang, J., Y. Xiao, K. Zhang, B. Luo, and C. Shen, Introducing Autoimmunity at the Synapse by a Novel Animal Model of Experimental Autoimmune Myasthenia Gravis. Neuroscience, 2018. 374: p. 264-270.
2. Liu, L., F. Xie, K. Wei, X.C. Hao, P. Li, J. Cao, and S. Min, Sepsis induced denervation-like changes at the neuromuscular junction. J Surg Res, 2016. 200(2): p. 523-32.
3. Allen, M.D., D.W. Stashuk, K. Kimpinski, T.J. Doherty, M.L. Hourigan, and C.L. Rice, Increased neuromuscular transmission instability and motor unit remodelling with diabetic neuropathy as assessed using novel near fibre motor unit potential parameters. Clin Neurophysiol, 2015. 126(4): p. 794-802.
4. Pleasure DE. Diseases Affecting Both the Peripheral and Central Nervous Systems. In: Siegel GJ, Agranoff BW, Albers RW, et al., editors. Basic Neurochemistry: Molecular, Cellular and Medical Aspects. 6th edition. Philadelphia: Lippincott-Raven; 1999. Available from: https://www.ncbi.nlm.nih.gov/books/NBK27985
5. Barrell, K., & Smith, A. G. (2018). Peripheral Neuropathy. Medical Clinics of North America. doi:10.1016/j.mcna.2018.10.006
6. Richardson, J. K., & Hurvitz, E. A. (1995). Peripheral Neuropathy: A True Risk Factor for Falls. The Journals of Gerontology Series A: Biological Sciences and Medical Sciences, 50A(4), M211–M215. doi:10.1093/gerona/50a.4.m211
7. Sibbald, R. G., & Ayello, E. A. (2019). Peripheral Neuropathy and the Insensate Foot. Advances in Skin & Wound Care, 32(4), 149. doi:10.1097/01.asw.0000554390.18232.bd
8. Pleasure DE. Examples of Peripheral Nervous System-Specific Diseases. In: Siegel GJ, Agranoff BW, Albers RW, et al., editors. Basic Neurochemistry: Molecular, Cellular and Medical Aspects. 6th edition. Philadelphia: Lippincott-Raven; 1999. Available from: https://www.ncbi.nlm.nih.gov/books/NBK28067/
9. Salzer JL. Schwann cell myelination. Cold Spring Harb Perspect Biol. 2015;7(8):a020529. Published 2015 Jun 8. doi:10.1101/cshperspect.a020529
10. Taetzsch, T. and G. Valdez, NMJ maintenance and repair in aging. Curr Opin Physiol, 2018. 4: p. 57-64.
11. Jones, R.A., C. Harrison, S.L. Eaton, M. Llavero Hurtado, L.C. Graham, L. Alkhammash, O.A. Oladiran, A. Gale, D.J. Lamont, H. Simpson, M.W. Simmen, C. Soeller, T.M. Wishart, and T.H. Gillingwater, Cellular and Molecular Anatomy of the Human Neuromuscular Junction. Cell Rep, 2017. 21(9): p. 2348- 2356.
12. Harris, K.P. and J.T. Littleton, Transmission, Development, and Plasticity of Synapses. Genetics, 2015. 201(2): p. 345-75.
13. Hyung, S., K. Jung, S.R. Cho, and N.L. Jeon, The Schwann Cell as an Active Synaptic Partner. Chemphyschem, 2018. 19(10): p. 1123-1127.
14. Arthur-Farraj, P.J., M. Latouche, D.K. Wilton, S. Quintes, E. Chabrol, A. Banerjee, A. Woodhoo, B. Jenkins, M. Rahman, M. Turmaine, G.K. Wicher, R. Mitter, L. Greensmith, A. Behrens, G. Raivich, R. Mirsky, and K.R. Jessen, c-Jun reprograms Schwann cells of injured nerves to generate a repair cell essential for regeneration. Neuron, 2012. 75(4): p. 633-47.
15. Kim, H.A., T. Mindos, and D.B. Parkinson, Plastic fantastic: Schwann cells and repair of the peripheral nervous system. Stem Cells Transl Med, 2013. 2(8): p. 553-7.
16. Aguayo, A.J., S. David, and G.M. Bray, Influences of the glial environment on the elongation of axons after injury: transplantation studies in adult rodents. J Exp Biol, 1981. 95: p. 231-40.

17. Webster, R.G., Animal Models of the Neuromuscular Junction, Vitally Informative for Understanding Function and the Molecular Mechanisms of Congenital Myasthenic Syndromes. Int J Mol Sci, 2018. 19(5).
18. Darabid, H., A.P. Perez-Gonzalez, and R. Robitaille, Neuromuscular synaptogenesis: coordinating partners with multiple functions. Nat Rev Neurosci, 2014. 15(11): p. 703-18.
19. Al-Ali H, Beckerman SR, Bixby JL, Lemmon VP. In vitro models of axon regeneration. Exp Neurol. 2017;287(Pt 3):423–434. doi:10.1016/j.expneurol.2016.01.020
20. Zervantonakis IK, Kothapalli CR, Chung S, Sudo R, Kamm RD. Microfluidic devices for studying heterotypic cell-cell interactions and tissue specimen cultures under controlled microenvironments. Biomicrofluidics. 2011;5(1):13406. Published 2011 Mar 30. doi:10.1063/1.3553237
21. Harris, K.P. and J.T. Littleton, Transmission, Development, and Plasticity of Synapses. Genetics, 2015. 201(2): p. 345-75.
22. Webster, R.G., Animal Models of the Neuromuscular Junction, Vitally Informative for Understanding Function and the Molecular Mechanisms of Congenital Myasthenic Syndromes. Int J Mol Sci, 2018. 19(5).
23. Arnold, A.S., M. Christe, and C. Handschin, A functional motor unit in the culture dish: co-culture of spinal cord explants and muscle cells. J Vis Exp, 2012(62).
24. Ionescu, A., E.E. Zahavi, T. Gradus, K. Ben-Yaakov, and E. Perlson, Compartmental microfluidic system for studying muscle-neuron communication and neuromuscular junction maintenance. Eur J Cell Biol, 2016. 95(2): p. 69-88.
25. Pourquie, O., Z. Al Tanoury, and J. Chal, The Long Road to Making Muscle In Vitro. Curr Top Dev Biol, 2018. 129: p. 123-142.
26. Dixon, T.A., E. Cohen, D.M. Cairns, M. Rodriguez, J. Mathews, R.R. Jose, and D.L. Kaplan, Bioinspired Three-Dimensional Human Neuromuscular Junction Development in Suspended Hydrogel Arrays. Tissue Eng Part C Methods, 2018. 24(6): p. 346-359.
27. McMacken, G., D. Cox, A. Roos, J. Muller, R. Whittaker, and H. Lochmuller, The beta-adrenergic agonist salbutamol modulates neuromuscular junction formation in zebrafish models of human myasthenic syndromes. Hum Mol Genet, 2018. 27(9): p. 1556-1564.
28. Abd Al Samid, M., J.S. McPhee, J. Saini, T.R. McKay, L.M. Fitzpatrick, K. Mamchaoui, A. Bigot, V. Mouly, G. Butler-Browne, and N. Al-Shanti, A functional human motor unit platform engineered from human embryonic stem cells and immortalized skeletal myoblasts. Stem Cells Cloning, 2018. 11: p. 85- 93.
29. Santhanam, N., L. Kumanchik, X. Guo, F. Sommerhage, Y. Cai, M. Jackson, C. Martin, G. Saad, C.W. McAleer, Y. Wang, A. Lavado, C.J. Long, and J.J. Hickman, Stem cell derived phenotypic human neuromuscular junction model for dose response evaluation of therapeutics. Biomaterials, 2018. 166: p. 64-78.
30. Santosa, K.B., A.M. Keane, A. Jablonka-Shariff, B. Vannucci, and A.K. Snyder-Warwick, Clinical relevance of terminal Schwann cells: An overlooked component of the neuromuscular junction. J Neurosci Res, 2018. 96(7): p. 1125-1135.
31. Cavaliere F, Benito-Muñoz M, Matute C. Organotypic Cultures as a Model to Study Adult Neurogenesis in CNS Disorders. Stem Cells Int. 2016;2016:3540568. doi:10.1155/2016/3540568
32. Al-Ali H, Beckerman SR, Bixby JL, Lemmon VP. In vitro models of axon regeneration. Exp Neurol. 2017;287(Pt 3):423–434. doi:10.1016/j.expneurol.2016.01.020

33. Cavaliere F, Benito-Muñoz M, Matute C. Organotypic Cultures as a Model to Study Adult Neurogenesis in CNS Disorders. Stem Cells Int. 2016;2016:3540568. doi:10.1155/2016/3540568
34. Tharin S, Kothapalli CR, Ozdinler PH, et al. A microfluidic device to investigate axon targeting by limited numbers of purified cortical projection neuron subtypes. Integr Biol (Camb). 2012;4(11):1398–1405. doi:10.1039/c2ib20019h
35. Langhammer, C.G., M.K. Kutzing, V. Luo, J.D. Zahn, and B.L. Firestein, Skeletal myotube integration with planar microelectrode arrays in vitro for spatially selective recording and stimulation: a comparison of neuronal and myotube extracellular action potentials. Biotechnol Prog, 2011. 27(3): p. 891-5.
36. Langhammer, C.G., M.K. Kutzing, V. Luo, J.D. Zahn, and B.L. Firestein, A topographically modified substrate-embedded MEA for directed myotube formation at electrode contact sites. Ann Biomed Eng, 2013. 41(2): p. 408-20.
37. Singh, T. and M. Vazquez, Time-Dependent Addition of Neuronal and Schwann Cells Increase Myotube Viability and Length in an In Vitro Tri-culture Model of the Neuromuscular Junction. Regen Eng Transl Med, 2019.
38. Cradock JC, et al. Evaluation of some pharmaceutical aspects of intrathecal methotrexate sodium, cytara-bine and hydrocortisone sodium succinate. American Journal of Hospital Pharmacy (1978); 35:402.
39. Campenot RB. Local control of neurite development by nerve growth factor. Proc Natl Acad Sci U S A. 1977;74(10):4516–4519. doi:10.1073/pnas.74.10.4516
40. Fantuzzo JA, De Filippis L, McGowan H, et al. μNeurocircuitry: Establishing in vitro models of neurocircuits with human neurons. Technology (Singap World Sci). 2017;5(2):87–97. doi:10.1142/S2339547817500054
41. Haines, C., & Goodhill, G. J. (2010). Analyzing neurite outgrowth from explants by fitting ellipses. Journal of Neuroscience Methods, 187(1), 52–58. doi:10.1016/j.jneumeth.2009.12.010
42. Andrew W. Fitzgibbon, Maurizio Pilu, and Robert B. Fisher. Direct least-squares fitting of ellipses, IEEE Transactions on Pattern Analysis and Machine Intelligence, 21(5), 476--480, May 1999
43. Singh, T., Robles, D., & Vazquez, M. (2020). Neuronal substrates alter the migratory responses of non-myelinating Schwann cells to controlled BDNF gradients. Journal of Tissue Engineering and Regenerative Medicine. doi:10.1002/term.3025
44. Jessen KR, Mirsky R. 2012. The Schwann cell lineage: Cellular transitions during development and after injury. In Neuroglia (ed. Kettenmann H, Ransom BR), pp. 159–171. Oxford University Press, Oxford.
45. Jessen KR, Mirsky R. 2005. The origin and development of glial cells in peripheral nerves. Nat Rev Neurosci 6: 671–682.
46. Jessen KR, Mirsky R, Lloyd AC. Schwann Cells: Development and Role in Nerve Repair. Cold Spring Harb Perspect Biol. 2015;7(7):a020487. Published 2015 May 8. doi:10.1101/cshperspect.a020487
47. Harty BL, Monk KR. Unwrapping the unappreciated: recent progress in Remak Schwann cell biology. Curr Opin Neurobiol. 2017;47:131–137. doi:10.1016/j.conb.2017.10.003
48. Webster HD. The geometry of peripheral myelin sheaths during their formation and growth in rat sciatic nerves. J Cell Biol. 1971;48(2):348–367. doi:10.1083/jcb.48.2.348
49. Thornton MR, Mantovani C, Birchall MA, Terenghi G. Quantification of N-CAM and N-cadherin expression in axotomized and crushed rat sciatic nerve. J Anat. 2005;206(1):69-78. doi:10.1111/j.0021-8782.2005.00369.x

50. Stewart, H. J. S., Turner, D., Jessen, K. R., & Mirsky, R. (1997). Expression and regulation of ?1?1 integrin in Schwann cells. Journal of Neurobiology, 33(7), 914–928. doi:10.1002/(sici)1097-4695(199712)33:7<914::aid-neu4>3.0.co;2-b
51. Jessen, K. R., & Mirsky, R. (2008). Negative regulation of myelination: Relevance for development, injury, and demyelinating disease. Glia, 56(14), 1552–1565. doi:10.1002/glia.20761
52. Sahenk, Z., Nagaraja, H. N., McCracken, B. S., King, W. M., Freimer, M. L., Cedarbaum, J. M., & Mendell, J. R. (2005). NT-3 promotes nerve regeneration and sensory improvement in CMT1A mouse models and in patients. Neurology, 65(5), 681–689. doi:10.1212/01.wnl.0000171978.70849.c5
53. Nave, K.-A., Sereda, M. W., & Ehrenreich, H. (2007). Mechanisms of Disease: inherited demyelinating neuropathies—from basic to clinical research. Nature Clinical Practice Neurology, 3(8), 453–464. doi:10.1038/ncpneuro0583
54. Taveggia C, Zanazzi G, Petrylak A, et al. Neuregulin-1 type III determines the ensheathment fate of axons. Neuron. 2005;47(5):681-694. doi:10.1016/j.neuron.2005.08.017
55. Michailov, G. V. (2004). Axonal Neuregulin-1 Regulates Myelin Sheath Thickness. Science, 304(5671), 700–703. doi:10.1126/science.109586
56. Willem, M., Garratt, A. N., Novak, B., Citron, M., Kaufmann, S., Rittger, A., … Haass, C. (2006). Control of Peripheral Nerve Myelination by the -Secretase BACE1. Science, 314(5799), 664–666. doi:10.1126/science.1132341
57. Topilko, P., Schneider-Maunoury, S., Levi, G., Baron-Van Evercooren, A., Chennoufi, A. B. Y., Seitanidou, T., … Charnay, P. (1994). Krox-20 controls myelination in the peripheral nervous system. Nature, 371(6500), 796–799. doi:10.1038/371796a0
58. Parkinson DB, Bhaskaran A, Droggiti A, et al. Krox-20 inhibits Jun-NH2-terminal kinase/c-Jun to control Schwann cell proliferation and death. J Cell Biol. 2004;164(3):385-394. doi:10.1083/jcb.200307132
59. Yoon C, Korade Z, Carter BD. Protein kinase A-induced phosphorylation of the p65 subunit of nuclear factor-kappaB promotes Schwann cell differentiation into a myelinating phenotype. J Neurosci. 2008;28(14):3738-3746. doi:10.1523/JNEUROSCI.4439-07.2008
60. Woodhoo A,Duran MB,Mirsky R,Jessen KR. 2007. Regulation of the immature phenotype by notch signaling. J Neuron Glia Biol 3: S13
61. Honjo T. 1996. The shortest path from the surface to the nucleus: RBP-J kappa/Su(H) transcription factor. Genes Cells 1: 1–9.
62. Doddrell RD, Dun XP, Moate RM, Jessen KR, Mirsky R, Parkinson DB. Regulation of Schwann cell differentiation and proliferation by the Pax-3 transcription factor. Glia. 2012;60(9):1269-1278. doi:10.1002/glia.22346
63. Kioussi C,Gross MK,Gruss P. 1995. Pax3: A paired domain gene as a regulator in PNS myelination. Neuron 15: 553–562.
64. Yang DP, Kim J, Syed N, et al. p38 MAPK activation promotes denervated Schwann cell phenotype and functions as a negative regulator of Schwann cell differentiation and myelination. J Neurosci. 2012;32(21):7158-7168. doi:10.1523/JNEUROSCI.5812-11.2012
65. Parkinson DB, Bhaskaran A, Arthur-Farraj P, et al. c-Jun is a negative regulator of myelination. J Cell Biol. 2008;181(4):625-637. doi:10.1083/jcb.200803013
66. Rotshenker S. Wallerian degeneration: the innate-immune response to traumatic nerve injury. J Neuroinflammation. 2011;8:109. Published 2011 Aug 30. doi:10.1186/1742-2094-8-109

67. Arthur-Farraj PJ, Latouche M, Wilton DK, et al. c-Jun reprograms Schwann cells of injured nerves to generate a repair cell essential for regeneration. Neuron. 2012;75(4):633-647. doi:10.1016/j.neuron.2012.06.021
68. Fontana X, Hristova M, Da Costa C, et al. c-Jun in Schwann cells promotes axonal regeneration and motoneuron survival via paracrine signaling. J Cell Biol. 2012;198(1):127-141. doi:10.1083/jcb.201205025
69. Hirata, K., & Kawabuchi, M. (2002). Myelin phagocytosis by macrophages and nonmacrophages during Wallerian degeneration. Microscopy Research and Technique, 57(6), 541–547. doi:10.1002/jemt.10108
70. Fu, S. Y., & Gordon, T. (1997). The cellular and molecular basis of peripheral nerve regeneration. Molecular Neurobiology, 14(1-2), 67–116. doi:10.1007/bf02740621
71. Parrinello S, Napoli I, Ribeiro S, et al. EphB signaling directs peripheral nerve regeneration through Sox2-dependent Schwann cell sorting. Cell. 2010;143(1):145-155. doi:10.1016/j.cell.2010.08.039
72. Allodi, I., Udina, E., & Navarro, X. (2012). Specificity of peripheral nerve regeneration: Interactions at the axon level. Progress in Neurobiology, 98(1), 16–37. doi:10.1016/j.pneurobio.2012.05.005
73. Sulaiman, O.A.R., Gordon, T., 2000. Effects of short- and long-term Schwann cell denervation on peripheral nerve regeneration, myelination, and size. Glia 32 (3), 234–246.
74. Li, Q., Ping, P., Jiang, H., & Liu, K. (2006). Nerve conduit filled with GDNF gene-modified schwann cells enhances regeneration of the peripheral nerve. Microsurgery, 26(2), 116–121. doi:10.1002/micr.20192
75. Politis, M.J., Spencer, P.S., 1981. A method to separate spatially the temporal sequence of axon-Schwann cell interaction during nerve regeneration. Journal of Neurocytology 10 (2), 221–232.
76. Martini, R., Xin, Y., Schmitz, B., Schachner, M., 1992. The L2/HNK-1 carbohydrate epitope is involved in the preferential outgrowth of motor neurons on ventral roots and motor nerves. European Journal of Neuroscience 4 (7), 628–639.
77. Saito, H., Nakao, Y., Takayama, S., Toyama, Y., Asou, H., 2005. Specific expression of an HNK-1 carbohydrate epitope and NCAM on femoral nerve Schwann cells in mice. Neuroscience Research 53 (3), 314–322
78. Martini, R., Schachner, M., Brushart, T.M., 1994. The L2/HNK-1 carbohydrate is preferentially expressed by previously motor axon-associated Schwann cells in reinnervated peripheral nerves. Journal of Neuroscience 14 (11 Pt 2), 7180– 7191.
79. Hoke, A., Redett, R., Hameed, H., Jari, R., Zhou, C., Li, Z.B., Griffin, J.W., Brushart, T.M., 2006. Schwann cells express motor and sensory phenotypes that regulate axon regeneration. Journal of Neuroscience 26 (38), 9646–9655.
80. Ma CH, Omura T, Cobos EJ, et al. Accelerating axonal growth promotes motor recovery after peripheral nerve injury in mice. J Clin Invest. 2011;121(11):4332-4347. doi:10.1172/JCI58675
81. Sulaiman, O. A. R., & Gordon, T. (2009). ROLE OF CHRONIC SCHWANN CELL DENERVATION IN POOR FUNCTIONAL RECOVERY AFTER NERVE INJURIES AND EXPERIMENTAL STRATEGIES TO COMBAT IT. Neurosurgery, 65(suppl_4), A105–A114. doi:10.1227/01.neu.0000358537.30354.63
82. Filipp ME, Travis BJ, Henry SS, et al. Differences in neuroplasticity after spinal cord injury in varying animal models and humans. Neural Regen Res. 2019;14(1):7-19. doi:10.4103/1673-5374.243694
83. Griffin, J. W., & Thompson, W. J. (2008). Biology and pathology of nonmyelinating Schwann cells. Glia, 56(14), 1518–1531. doi:10.1002/glia.20778

84. Negro S, Lessi F, Duregotti E, et al. CXCL12α/SDF-1 from perisynaptic Schwann cells promotes regeneration of injured motor axon terminals. EMBO Mol Med. 2017;9(8):1000-1010. doi:10.15252/emmm.201607257
85. Burns, A. S., Jawaid, S., Zhong, H., Yoshihara, H., Bhagat, S., Murray, M., … Son, Y.-J. (2006). Paralysis elicited by spinal cord injury evokes selective disassembly of neuromuscular synapses with and without terminal sprouting in ankle flexors of the adult rat. The Journal of Comparative Neurology, 500(1), 116–133. doi:10.1002/cne.21143
86. Painter MW, Brosius Lutz A, Cheng YC, et al. Diminished Schwann cell repair responses underlie age-associated impaired axonal regeneration. Neuron. 2014;83(2):331-343. doi:10.1016/j.neuron.2014.06.016